Mechanics & Industry **20**, 502 (2019)
© AFM, EDP Sciences 2019
https://doi.org/10.1051/meca/2019022

Mechanics & Industry

Available online at:
www.mechanics-industry.org

Regular Article

Influence of rotating magnetic field on Maxwell saturated ferrofluid flow over a heated stretching sheet with heat generation/absorption

Aaqib Majeed[1,*], Ahmed Zeeshan[2], Farzan Majeed Noori[3], and Usman Masud[4]

[1] Departmentof Mathematics Statistics, Bacha Khan University, 24420 Charsadda, KPK, Pakistan
[2] Department of Mathematics and Statistics, FBAS, IIUI, H-10, Islamabad 44000, Pakistan
[3] Department of Informatics, Faculty of Mathematics and Natural Sciences, University of Oslo, Oslo, Norway
[4] Department of Electronic Engineering, University of Engineering and Technology, Taxila, Pakistan

Received: 29 January 2018 / Accepted: 22 March 2019

Abstract. This article is focused on Maxwell ferromagnetic fluid and heat transport characteristics under the impact of magnetic field generated due to dipole field. The viscous dissipation and heat generation/absorption are also taken into account. Flow here is instigated by linearly stretchable surface, which is assumed to be permeable. Also description of magneto-thermo-mechanical (ferrohydrodynamic) interaction elaborates the fluid motion as compared to hydrodynamic case. Problem is modeled using continuity, momentum and heat transport equation. To implement the numerical procedure, firstly we transform the partial differential equations (PDEs) into ordinary differential equations (ODEs) by applying similarity approach, secondly resulting boundary value problem (BVP) is transformed into an initial value problem (IVP). Then resulting set of non-linear differentials equations is solved computationally with the aid of Runge–Kutta scheme with shooting algorithm using MATLAB. The flow situation is carried out by considering the influence of pertinent parameters namely ferro-hydrodynamic interaction parameter, Maxwell parameter, suction/injection and viscous dissipation on flow velocity field, temperature field, friction factor and heat transfer rate are deliberated via graphs. The present numerical values are associated with those available previously in the open literature for Newtonian fluid case ($\gamma_1 = 0$) to check the validity of the solution. It is inferred that interaction of magneto-thermo-mechanical is to slow down the fluid motion. We also witnessed that by considering the Maxwell and ferrohydrodynamic parameter there is decrement in velocity field whereas opposite behavior is noted for temperature field.

Keywords: Maxwell ferrofluid / rotating magnetic field / heat generation / heat absorption / viscous dissipation / suction / injection

1 Introduction

Boundary layer theory by Prandtl confirmed to be greatly used in the flow of Newtonian fluids as the Navier–Stokes equations can be reduced to simpler equations. Such flow along with heat transfer analysis has acknowledged extensive attention in current decays because of their momentous contribution in industry. A few of applications are found like hot rolling, continuous casting of metals, glass blowing, cooling of an infinite metallic plate in a cooling bath, metal spinning and the aerodynamic extrusion of plastic sheets. The concept on boundary layer flow of over a continuously moving surface was initiated by Sakiadis [1]. The pioneer work of Sakiadis has been extended by many researchers for various physical aspect of the problem [2–6]. Furthermore, the industrial use of non-Newtonian fluids with heat transport analysis inspires the scientists and engineers in the research field. Industrial processes like in polymer depolarization, processing, composite, fermentation, bubble columns and absorption, boiling and lubrication which shows the consequence of non-Newtonian liquids in industries. Numerous models of non-Newtonian fluids describe different fluid behaviors exists. Maxwell fluid is one of such type fluid which is exclusive valuable for polymers for low molecular weight. Many mathematicians and scientists studied the behavior of Maxwell's liquid flow. Nadeem et al. [7] described

* e-mail: aaqib@bkuc.edu.pk

numerical investigations of nanofluid over a stretching surface by utilizing Maxwell model. Majeed et al. [8] described magneto-hydrodynamic (MHD) effect on stagnation point of Maxwell liquid flow due to stretched surface by applying homotopy analytical method (HAM). Hayat and Qasim [9] have examined chemical reaction and heat transport analysis of Maxwell ferromagnetic liquid flow toward a stretching sheet with the effects of Soret and suction. Aliakbar et al. [10] have investigated the radiation effect on MHD flow of Maxwellian liquids over a stretching surface. But these studies do not incorporate the heat transfer and heat absorption effects. Bataller [11] discussed radiation and heat source/sink impact on viscoelastic fluid flow and heat transport phenomena past a stretchable surface. Abel et al. [12] analyzed the combine impact of magnetic field and viscous dissipation on viscoelastic liquid flow due to stretched surface. Rashidi et al. [13] have obtained analytical approximate boundary layer solution of electrically conducting two-dimensional viscoelastic liquid flow over a moving surface. Majeed et al. [14] performed the heat transfer analysis of magneto-Eyring–Powell fluid flow over a stretchable surface with multiple slip effects and variable transverse magnetic field.

Ferrofluids (magnetic nanofluids) are liquids which are vastly magnetized under the impact of applied magnetic field. These fluids were first industrialized by Papell [15] at NASA in 1963. In ferrofluids, non-magnetic carrier fluids are saturated with micron-sized colloidal ferrous particles uniformly distributed [16]. The fluid shows remarkable applications other than in rocket fuel. These are used in shock absorbers, coolers of nuclear reactor, MEMS, microfluidic actuators, leak-proof seals, lithographic designing and much more [17–21]. Neuringer [22] demonstrated stagnation point flow of ferromagnetic liquid flow toward a cold wall along with surface temperature declines linearly. Sheikholeslami and Gorji-Bandpy [23] reported the flow of ferrofluid in a heated cavity from beneath with the impact of magnetic field. Rehman et al. [24] investigated theoretically 2D boundary layer flow of Maxwell ferromagnetic fluid over a flat plate under the impact of two equal magnetic dipole and Cattaneo–Christov flux model. Hassan et al. [25] examined the nanoparticle shape effects on ferrofluids flow and heat transfer in the presence of low oscillating magnetic field. Feng et al. [26] examined experimental study for controlling heat transport characteristics of ferrofluid. Rashidi et al. [27] discussed the mixed convection flow of magnetic nanofluid flow in a channel with sinusoidal walls. Sheikholeslami and Gorji-Bandpy [28] investigated numerically ferrofluid flow in a cavity under the impact of applied magnetic field. Some of the literature related to ferromagnetic liquid flow because dipole field were executed by the scientist in the set [29–38].

Literature survey discloses that a lot of work has been done by several researchers to explore the heat transfer characteristic on boundary layer stretched flows. But the main theme of the present investigations is to discuss the heat generation or absorption effect on boundary layer Maxwell ferromagnetic liquid flow with the existence of point dipole field which has not been studied so far. The modelled equations of flow problem consisting of momentum and thermal transport are converted to a nonlinear ordinary differential equations (ODEs) using suitable similarity approach and then solve by Runge–Kutta (R–K) method. The influence of various constraints is discussed in detail through graphs.

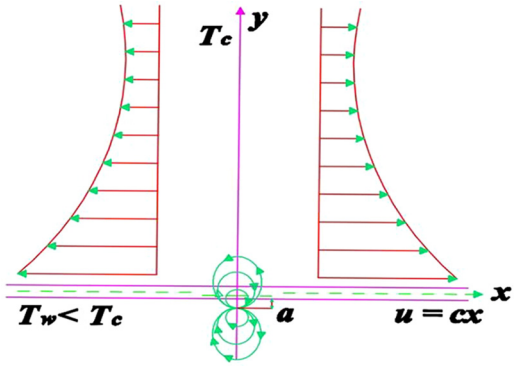

Fig. 1. Geometry of the problem.

2 Mathematical model

2.1 Magnetic field due to dipole

Flow of magnetic fluid influenced due to dipole field (see Fig. 1) and ψ represents the scalar potential of dipole magnetic field, which are

$$\psi = \frac{\chi}{2\pi}\left(\frac{x}{x^2+(y+a)^2}\right), \tag{1}$$

and components of magnetic field H are

$$H_x = -\frac{\partial\psi}{\partial x} = \frac{\chi}{2\pi}\left[\frac{x^2-(y+a)^2}{\left(x^2+(y+a)^2\right)^2}\right], \tag{2}$$

$$H_y = -\frac{\partial\psi}{\partial y} = \frac{\chi}{2\pi}\left[\frac{2x(y+a)}{\left(x^2+(y+a)^2\right)^2}\right]. \tag{3}$$

Magnetic body force and gradient of H are proportional to each other, we get:

$$H = \sqrt{\left(\frac{\partial\psi}{\partial x}\right)^2+\left(\frac{\partial\psi}{\partial y}\right)^2}. \tag{4}$$

In component form, we have

$$\frac{\partial H}{\partial x} = -\frac{\chi}{2\pi}\left[\frac{2x}{(y+a)^4}\right], \tag{5}$$

$$\frac{\partial H}{\partial y} = \frac{\chi}{2\pi}\left[\frac{-2}{(y+a)^3}+\frac{4x^2}{(y+a)^5}\right]. \tag{6}$$

The representation of magnetization M is taken in the form of linear temperature as [39]

$$M = K^*(T_c - T). \tag{7}$$

2.2 Flow analysis

Here, we consider 2D incompressible electrified Maxwell ferromagnetic liquid flow under the influence of line dipole over a linear permeable sheet. Sheet is stretched with u_w and perpendicular to y-axis as shown Figure 1. A magnetic dipole is located at distance "a" with its center is on y-axis. Due to dipole, the direction of magnetic fluid in the +ve x-direction gives rise to magnetic field of appropriate strength to drench the ferromagnetic fluid. Here, wall temperature is T_w and Curie temperature is T_c, whereas the free stream temperature away from the wall is $T_\infty = T_c$. Under Boussinesq's condition, the governing flow equations in the presence of magnetic dipole are:

$$\frac{\partial u}{\partial x} + \frac{\partial v}{\partial y} = 0, \tag{8}$$

$$u\frac{\partial u}{\partial x} + v\frac{\partial u}{\partial y} + \lambda_1\left(u^2\frac{\partial^2 u}{\partial x^2} + v^2\frac{\partial^2 u}{\partial y^2} + 2uv\frac{\partial^2 u}{\partial x \partial y}\right) = \frac{\mu_0}{\rho}M\frac{\partial H}{\partial x} + \nu\frac{\partial^2 u}{\partial y^2}, \tag{9}$$

$$\rho c_p\left(u\frac{\partial T}{\partial x} + v\frac{\partial T}{\partial y}\right) + \mu_0 T\frac{\partial M}{\partial T}\left(u\frac{\partial H}{\partial x} + v\frac{\partial H}{\partial y}\right) = k\frac{\partial^2 T}{\partial y^2} + \mu\left[2\left(\frac{\partial u}{\partial x}\right)^2 + 2\left(\frac{\partial v}{\partial y}\right)^2 + \left(\frac{\partial v}{\partial x} + \frac{\partial u}{\partial y}\right)^2\right] - Q_0(T_c - T), \tag{10}$$

with boundary conditions are

$$u = u_w = cx, v = v_w, T = T_w = T_c - A\left(\frac{x}{l}\right)^2 \quad \text{at} \quad y = 0, \tag{11}$$

$$u \to 0, \frac{\partial u}{\partial y} \to 0, T \to T_c, \text{as} \quad y \to \infty. \tag{12}$$

Here, $c > 0$ signify the rate of stretching sheet, A is constant, v_w represents the suction/injection velocity and $l = \sqrt{\nu/c}$ is characteristic length.

3 Solution of the problem

We introduce the non-dimensional stream function $\varphi(\xi, \eta)$ and temperature $\theta(\xi, \eta)$ assumed by [39].

$$\phi(\xi, \eta) = \left(\frac{\mu}{\rho}\right)\xi.f(\eta), \theta(\xi, \eta) = \frac{T_c - T}{T_c - T_w} = \theta_1(\eta) + \xi^2\theta_2(\eta). \tag{13}$$

Here, $T_c - T_w = A\left(\frac{x}{l}\right)^2$, (ξ, η) are the non-dimensional component of φ

$$\xi = \sqrt{\frac{c\rho}{\mu}}x, \eta = \sqrt{\frac{c\rho}{\mu}}y. \tag{14}$$

Velocity components are:

$$u = \frac{\partial \phi}{\partial y} = cx.f'(\eta), v = -\frac{\partial \phi}{\partial x} = -\sqrt{c\nu}.f(\eta). \tag{15}$$

Putting equations (13)–(15) into equations (9) and (10), and obtain the expression up to the power of ξ^2, we get:

$$f'''(1 - \gamma_1 f^2) - \left(f'^2 - ff''\right) + 2\gamma_1 ff'f'' - \frac{2\beta\theta_1}{(\eta + \alpha_1)^4} = 0, \tag{16}$$

$$\theta''_1 + Pr(f\theta_1' - 2f'\theta + Q\theta_1) + \frac{2\lambda\beta(\theta_1 - \varepsilon)f}{(\eta + \alpha_1)^3} - 2\lambda f'^2 = 0, \tag{17}$$

$$\theta''_2 - Pr(4f'\theta_2 - f\theta_2' - Q\theta_1) + \frac{2\lambda\beta\theta_2 f}{(\eta + \alpha_1)^3} - \lambda\beta(\theta_1 - \varepsilon)\left[\frac{2f'}{(\eta + \alpha_1)^4} + \frac{4f}{(\eta + \alpha_1)^5}\right] - \lambda f''^2 = 0. \tag{18}$$

Correspondig boundary relations (11) and (12) takes the form

$$\left.\begin{aligned} &f(0) = S, f'(0) = 1, \theta_1(0) = 1, \theta_2(0) = 0, \\ &f'(\infty) = 0, \theta_1(\infty) = 0, \ \theta_2(\infty) = 0. \end{aligned}\right\} \tag{19}$$

The pertinent parameter appearing in the above equations (16)–(18) are

$$\left.\begin{aligned} &\beta = \frac{\chi\rho}{2\pi\mu^2}\mu_0 K^*(T_c - T_w), \gamma_1 = \lambda_1 c, \lambda = \frac{c\mu^2}{\rho k(T_c - T_w)}, \\ &Pr = \frac{\mu c_p}{k}, S = \frac{-v_w}{\sqrt{c\nu}}, \alpha_1 = \sqrt{\frac{c\rho}{\mu}}a, \varepsilon = \frac{T_c}{T_c - T_w}, Q = \frac{Q_0}{\rho c_p} \end{aligned}\right\}. \tag{20}$$

4 Quantities of physical interest

Skin friction and heat transfer rate are stated as

$$C_{fx} \equiv \frac{-2\tau_w}{\rho(cx)^2}; \tau_w = \mu\left(\frac{\partial u}{\partial y}\right)_{y=0}, \tag{21}$$

and

$$\mathrm{Nu}_x \equiv \frac{xq_w}{-k(T_c - T_w)}; q_w = -k\left(\frac{\partial T}{\partial y}\right)_{y=0}. \tag{22}$$

Using the equations (13)–(15) we get

$$\begin{aligned} C_f Re_x^{1/2} &= -2f''(0), \mathrm{Nu}_x/Re_x^{1/2} \\ &= -\left(\theta_1{}'(0) + \xi^2\theta_2{}'(0)\right), \end{aligned} \tag{23}$$

where $Re_x = \frac{\rho c x^2}{\mu}$ refer local Reynolds number. It is more attractive and appropriate to exchange the non-dimension Nusselt number $-\theta' = -\left[\theta'_1(0) + \xi^2\theta'_2(0)\right]$ with the distance free from ξ, obtained a ratio $\theta^*(0) = \frac{\theta_1{}'(0)}{\theta_1{}'(0)|_{\beta=0}}$ termed as heat transfer rate as sheet.

5 Numerical scheme

In this sections, we have solved equations (16)–(18) with corresponding boundary conditions (19). It is tough to find analytical solution, so to overcome this complexity, we solve it numerically. For this R–K based shooting method is used with the aid of Matlab package for numerous set of pertinent parameters β, Pr, S, γ_1, Q and λ. The set of coupled PDEs is transformed into differential equations for seven unknowns which are solved as an initial value problem (IVP). Let $z_1 = f$, $z_2 = f'$, $z_3 = f''$, $z_4 = \theta_1$, $z_5 = \theta_1{}'$, $z_6 = \theta_2$, $z_7 = \theta_2{}'$. By introducing these new constraints in the equations (16)–(22) we obtain:

See equations (24) below.

Since $z_3(0)$, $z_5(0)$ and $z_7(0)$ are not mentioned, so we establish initial guesses start with $z_3(0) = w_{10}$, $z_5(0) = w_{20}$ and $z_7(0) = w_{30}$. Let χ_1, χ_2 and χ_3 be the correct estimation of $z_3(0)$, $z_5(0)$ and $z(0)$, respectively. The final form of ODEs is solved by utilizing R–K scheme and signifies the values of z_3, z_5 and z_7 at $\eta = \eta_\infty$ by $z_3(w_{10}, w_{20}, w_{30}, \eta_\infty)$, $z_5(w_{10}, w_{20}, w_{30}, \eta_\infty)$ and $z_7(w_{10}, w_{20}, w_{30}, \eta_\infty)$, respectively. Meanwhile y_3, y_5 and y_7 are obviously a function of χ_1, χ_2 and χ_3, they have opened in Taylor series around $\chi_1 - w_{10}$, $\chi_2 - w_{20}$ and $\chi_3 - w_{30}$, only linear terms survive. The treatment of difference quotients is made for the derivatives appeared in these Taylor series expansions. Thus, after resolving the set of Taylor series expansions for $\delta\chi_1 = \chi_1 - w_{10}$, $\delta\chi_2 = \chi_2 - w_{20}$ and $\delta\chi_3 = \chi_3 - w_{30}$, we obtain the new guess $w_{11} = w_{10} + \delta w_{10}$, $w_{21} = w_{20} + \delta w_{20}$ and $w_{31} = w_{30} + \delta w_{30}$. Following, process is repeated starting with $z_1(0)$, $z_2(0)$, w_{11}, $z_4(0)$, w_{21}, $y_5(0)$ and w_{31} is considered as initial values. The overall iteration procedure is recurring with most current values of χ_1, χ_2 and χ_3 until we fulfill the required boundary conditions.

Lastly $w_{1n} = w_{1(n-1)} + \delta w_{1(n-1)}$, $w_{2n} = w_{2(n-1)} + \delta w_{2(n-1)}$ and $w_{3n} = w_{3(n-1)} + \delta w_{3(n-1)}$ for $n = 1, 2, 3, \ldots$ are achieved which appeared to be the most preferred approximate initial values of $z_3(0)$, $z_5(0)$ and $z_7(0)$. So, in this way, we obtained all initial conditions. Now it is possible to solve the set of ODEs by R–K method so that the required field for a definite set of convergence parameters can simply establish with error is chosen to be 10^{-5} in order to obtain the best convergence.

6 Graphical outcomes

In this segment, we have investigated the performance of physical parameters with the assistance of graphs and table. The graphical outcomes are displayed for dimensionless velocity profile, temperature profile, Nusselt number, and skin friction against MHD interaction parameter, Maxwell parameter, heat generation or absorption, viscous dissipation, Prandtl number and suction or injection parameter. For computational work, the value of the controlling parameters is considered as $Pr = 7.0$, $\beta = 0.1$, $\gamma_1 = 0.2$, $\lambda = 0.01$, $S = 0.1$, $Q = 0.1$, $\varepsilon = 2.0$, $\alpha_1 = 1.0$. To validate and confirm the accuracy of the present numerical procedure, our current results of local Nusselt number $-\theta_1{}'(0)$ in case of Newtonian fluid ($\gamma_1 = 0$) are compared with the existing data of Chen [6] and Abel

$$\begin{bmatrix} z'_1 \\ z'_2 \\ z'_3 \\ z'_4 \\ z'_5 \\ z'_6 \\ z'_7 \end{bmatrix} = \begin{bmatrix} z_2, \\ z_3, \\ \dfrac{1}{\left(1-\gamma_1 z_1^2\right)}\left[\left(z_2^2 - z_1 z_3\right) - 2\gamma_1 z_2 z_3 + \dfrac{2\beta z_4}{(\eta+\alpha_1)^4}\right], \\ z_5, \\ -Pr(z_1 z_5 - 2z_2 z_4 - Q z_4) - \dfrac{2\lambda\beta z_1(z_4-\varepsilon)}{(\eta+\alpha_1)^3} + 2\lambda z_2^2 \\ z_7, \\ Pr(4z_2 z_6 - z_1 z_7 - Q z_6) - \dfrac{2\lambda\beta z_1 z_6}{(\eta+\alpha_1)^3} - \lambda\beta(z_4-\varepsilon)\left[\dfrac{2z_2}{(\eta+\alpha_1)^4} + \dfrac{4z_1}{(\eta+\alpha_1)^5}\right] + \lambda z_3^2 \end{bmatrix}. \tag{24}$$

Table 1. Calculation of Nusselt number $-\theta_1'(0)$, when $\beta=\lambda=\gamma_1=S=Q=0$.

Pr	Chen [6]	Abel et al. [12]	Present results
0.72	1.0885	1.0885	1.088527
1	1.3333	1.3333	1.333333
3	2.5097	–	2.509725
10	4.7968	4.7968	4.796873

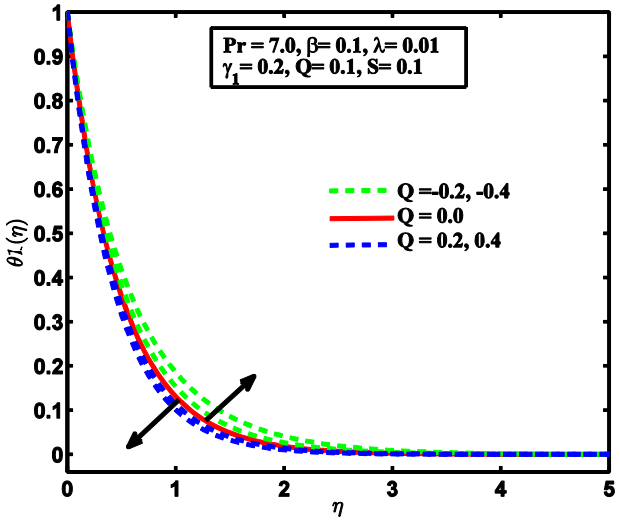

Fig. 2. Impact of Q on temperature profile.

et al. [12] for different values of Prandtl number are presented in Table 1, and found a superb accuracy with the publicized data.

Figure 2 is drawn for velocity field against heat generation/absorption parameter Q. From the outcomes, it is examined that energy boundary layer thickness rises for $Q>0$ due to increasing in the thermal state of the fluid. From a physical characteristic heat source in thermal boundary layer produces energy, because of this fact temperature increases with the increase of Q. This increment in temperature provides an increase in flow field. Conversely, with the occurrence of heat absorption, there occurs decrement in the temperature field for $Q<0$, so producing decrement in thermal boundary layer as seen in Figure 2.

Figures 3 and 4 represent the establishment of variation of sanction/injection parameter on the flow fields. It is noticed that when suction parameter is $S>0$ fluid velocity reduces significantly whereas velocity of the fluid is increased for injection $S<0$. Figure 4 points out that thermal boundary layer thickness diminishes by intensifying the suction parameter and increases the temperature profile due to injection parameter because temperature is overshoot for injection $S<0$. This feature overcomes up to a specific height and afterward the procedure slows down and at distance away from the surface temperature vanishes.

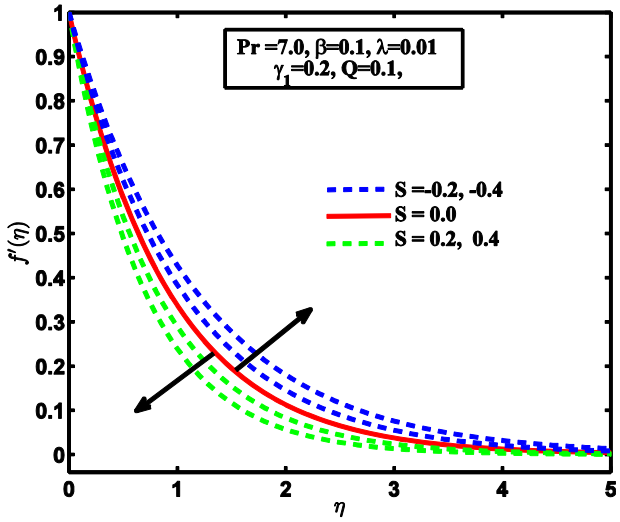

Fig. 3. Impact of S on velocity distribution.

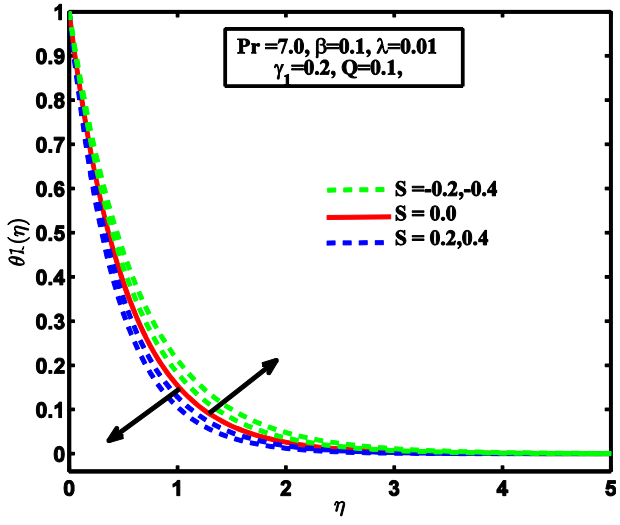

Fig. 4. Impact of S temperature profile.

The impact of ferromagnetic on problem is considered by taking ferro-hydrodynamic interaction parameter β and dimensionless distance between the center of the magnetic dipole and origin. From physical point of view there is an interaction between the fluid motion and the external magnetic field due to dipole. Consequently enhancement in ferromagnetic parameter β leads to flattening the axial velocity$f'(\eta)$. In fact, ferromagnetic fluid fundamentally has a transporter liquid flow with tinny size ferrite particles which improve the viscosity of the liquid, and therefore velocity profile reduces for higher value of β transfer of heat is also improved via decay motion. It is more fascinating to perceive that due to impact of magnetic dipole, fluid velocity remains lower as compared to MHD case ($\beta=0$) as shown in Figure 5. Since there is an interference among the motion of fluid and the stroke of point dipole. This type of

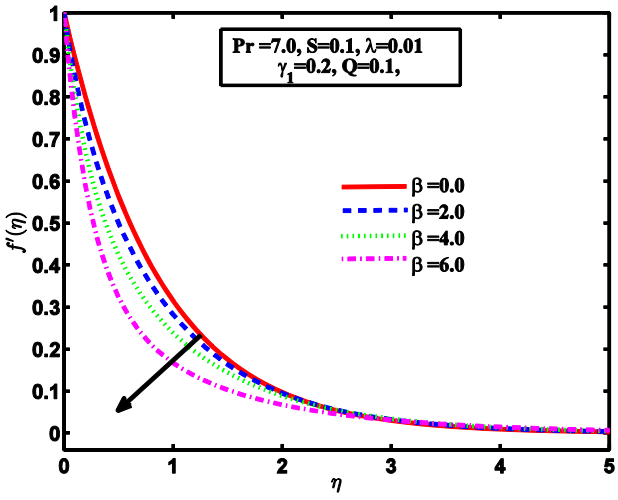

Fig. 5. Impact of β on velocity profile.

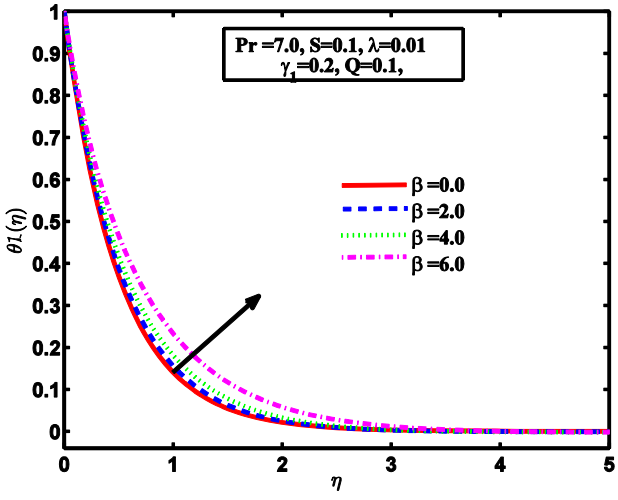

Fig. 6. Impact of β on temperature profile.

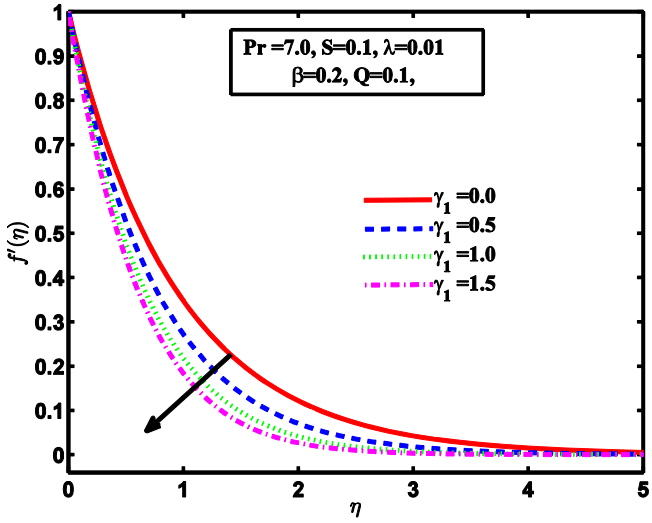

Fig. 7. Impact of γ_1 on velocity profile.

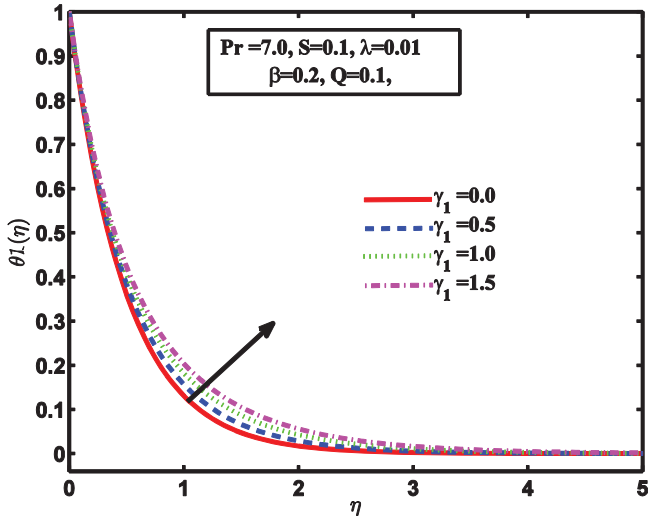

Fig. 8. Impact of γ_1 on temperature profile.

intervention slows down the fluid velocity and increases the frictional heating involving inside the fluid layers which are responsible for the improvement in the energy transport as cleared in Figure 6.

Figures 7 and 8 are outlined for velocity and temperature profile versus Maxwell parameter γ_1. From graphs it is concluded that an increase in Maxwell parameter γ_1 is to decline fluid velocity overhead the surface, and associated boundary layer thickness is decreased for a large value of γ_1. From physical view point, when shear stress is detached fluid will come to rest. These sorts of philosophy are revealed in many cases of polymeric fluids which are not clear in the Newtonian model. For higher value Maxwell parameter will produce a retarding force between two adjacent layers which develop a suppression in the fluid velocity and momentum boundary layer thickness as shown in Figure 7. Also, perceived that temperature profile increases by the large value of Maxwell parameter, since thermal boundary layer thickness grows into broadened when we enhance Maxwell parameter as illustrated in Figure 8. Therefore, the cooling of a heated sheet can be enhanced by picking a coolant having a small Maxwell parameter. The consequence of frictional heating because of viscosity and magnetic dipole on temperature field is signified by dissipation parameter λ. Figure 9 simply demonstrates the influence of λ on temperature profile. Result describes that temperature is decreased by enlarging the value of λ. This happens due to extraordinary behavior of ferrofluid on boundary layer transport. On the other end, this is contradictory in the case of hydrodynamic ($\beta = 0$) whereas increasing in the value of λ shows an increment in temperature profile near the boundary layer region.

Figures 10 and 11 are plotted to see the impact of suction parameter on local Nusselt and skin friction coefficient versus ferromagnetic interaction parameter. Given result shows skin friction enhancement for numerous values of ferromagnetic interaction parameter and suction

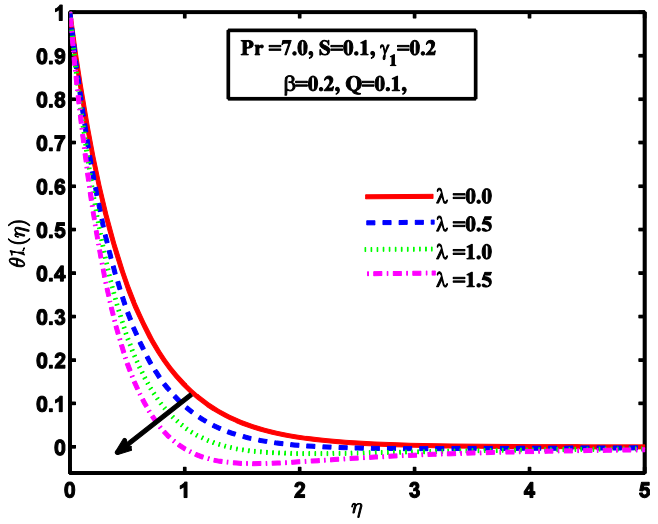

Fig. 9. Impact of λ on temperature profile.

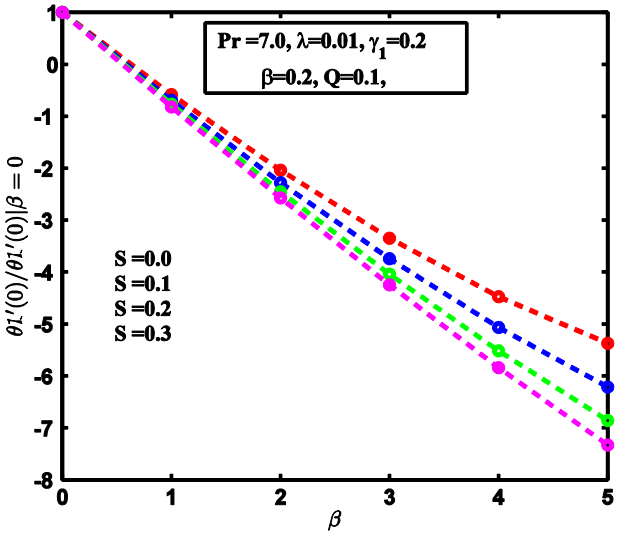

Fig. 11. Impact of S and β on Nusselt number.

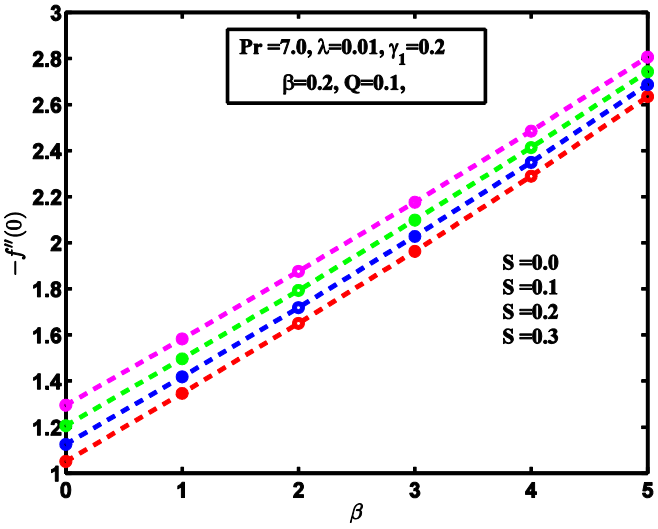

Fig. 10. Impact of S and β on skin friction coefficient.

parameter. This behavior appears because of external magnetic field which produced a drag force known as Lorentz force. Due to this force, fluid velocity is depressed and hence increasing skin friction coefficient, but inverse trend is noted for Nusselt number as shown in Figure 11.

7 Closing remarks

In the present study, impact of heat generation or absorption on Maxwell ferromagnetic liquid flow due to stretched surface affected by magnetic dipole field with suction or injection parameter. Mathematical PDEs of momentum and energy are first converted into ODEs, then solved by adopting R–K based shooting procedure using MATLAB package. Some effective governing parameters on the flow problem like Maxwell parameter (γ_1), ferromagnetic interaction parameter (β), viscous dissipation parameter (λ), heat generation or absorption parameter (Q), sanction or injection parameter (S) on velocity, temperature, skin friction and heat transfer rate are explained graphically and discussed. Some of the major observations of the current flow problem are summarized as below:

- Impact of both suction and ferromagnetic parameter is to suppress the fluid velocity which causes the improvement in skin-friction coefficient.
- Nusselt number is reduced by rising the ferromagnetic interaction parameter.
- The influence of Maxwell parameter is to decrease the velocity profile and enhance the temperature profile in the region of boundary layer.

Nomenclature

a	Distance
c	Stretching rate
c_p	Specific heat transfer ($\mathrm{J\,kg^{-1}\,K^{-1}}$)
C_{f_x}	Skin friction coefficient
k	Thermal conductivity ($\mathrm{W\,m^{-1}\,K^{-1}}$)
H	Magnetic field (A/m)
Nu_x	Local Nusselt number
K^*	Pyromagnetic coefficient
M	Magnetization (A/m)
Q	Heat generation/absorption
Re_x	Reynold number
S	Suction/injection parameter
T	Fluid temperature (K)
$(u,\ v)$	Velocity components ($\mathrm{m\,s^{-1}}$)
$(x,\ y)$	Cartesian coordinates (m)
μ	Dynamic viscosity
μ_0	Magnetic permeability
l	Characteristic length
Pr	Prandtl number
v_w	Wall mass flux
T_c	Curie temperature (K)

Greek symbols

ρ Density ($\mathrm{kg\,m^{-3}}$)
ψ Scalar magnetic potential
ϕ Stream function ($\mathrm{m^2\,s^{-1}}$)
δ Slip parameter
ε Curie temperature
τ_w Shear stress
λ Viscous dissipation parameter
λ_1 Relaxation time
α_1 Non-dimensional distance
β Ferromagnetic interaction parameter
χ Strength of magnetic field (A/m)
γ_1 Maxwell parameter

References

[1] B.C. Sakiadis, Boundary layer behavior on continuous solid surface: I. Boundary-layer equations for two-dimensional and axisymmetric flow, AIChE J. 7 (1961) 26–34
[2] T.C. Chiam, Hydromagnetic flow over a surface stretching with a power-law velocity, Int. J. Eng. Sci. 33 (1995) 429–435
[3] S. Liao, I. Pop, Explicit analytic solution for similarity boundary layer equations, Int. J. Heat Mass Transf. 47 (2004) 75–85
[4] L.J. Grubka, K.M. Bobba, Heat transfer characteristics of a continuous stretching surface with variable temperature, J. Heat Transfer. 107 (1985) 248–250
[5] B.K. Dutta, P. Roy, A.S. Gupta, Temperature field in flow over a stretching surface with uniform heat flux, Int. Commun. Heat Mass Transf. 12 (1985) 89–94
[6] C.H. Chen, Laminar mixed convection adjacent to vertical, continuously stretching sheets, Heat Mass Transf. 33 (1998) 471–698
[7] S. Nadeem, R. Mehmood, N.S. Akbar, Non-orthogonal stagnation point flow of a nano non-Newtonian fluid towards a stretching surface with heat transfer. Int. J. Heat Mass Transf. 57 (2013) 679–689
[8] A. Majeed, A. Zeeshan, R. Ellahi, Chemical reaction and heat transfer on boundary layer Maxwell Ferro-fluid flow under magnetic dipole with Soret and suction effects, Eng. Sci. Technol. Int. J. 20 (2017) 1122–1128
[9] T. Hayat, M. Qasim, Influence of thermal radiation and joule heating on MHD flow of a Maxwell fluid in the presence of thermophoresis, Int. J. Heat Mass Transf. 53 (2010) 4780–4788
[10] V. Aliakbar, A.A. Pahlavan, K. Sadeghy, The influence of thermal radiation on MHD flow of Maxwellian fluids above stretching sheets, Commun. Nonlinear Sci. Numer. Simul. 14 (2009) 779–794
[11] R.C. Bataller, Effects of heat source/sink, radiation and work done by deformation on flow and heat transfer of a viscoelastic fluid over a stretching sheet, Comput. Math. Appl. 53 (2007) 305–316
[12] M.S. Abel, E. Sanjayanand, M.M. Nandeppanavar, Viscoelastic MHD flow and heat transfer over a stretching sheet with viscous and ohmic dissipations, Commun. Nonlinear Sci. Numer. Simul. 13 (2008) 1808–1821
[13] M.M. Rashidi, E. Momoniat, B. Rostami, Analytic approximate solutions for MHD boundary-layer viscoelastic fluid flow over continuously moving stretching surface by Homotopy Analysis Method with two auxiliary parameters, J. Appl. Math. 2012 (2012) 19
[14] A. Majeed, A. Zeeshan, H. Xu, M. Kashif, U. Masud, Heat transfer analysis of magneto-Eyring-Powell fluid over a nonlinear stretching surface with multiple slip effects: Application of Roseland's heat flux, Can. J. Phys. (2019), doi: 10.1139/cjp-2018-0602
[15] S.S. Papell, Low viscosity magnetic fluid obtained by the colloidal suspension of magnetic particles, US-PATENT-APPL-SN-315096
[16] R.E. Rosensweig, Ferrohydrodynamics, Dover Publications, Inc., New York, 1997
[17] A. Jafari, T. Tynjala, S. Mousavi, P. Sarkomaa, Cfd simulation and evaluation of controllable parameters effect on thermomagnetic convection in ferrofluids using Taguchi technique, Comput. Fluids 37 (2008) 1344–1353
[18] F. Selimefendigil, H.F. Oztop, Numerical study and pod-based prediction of natural convection in ferrofluids filled triangular cavity with generalized neural networks, Numer. Heat Transf. A: Appl. 67 (2015) 1136–1161
[19] P. Bissell, P. Bates, R. Chantrell, K. Raj, J. Wyman, Cavity magnetic field measurements in ferrofluids, J. Magn. Magn. Mater. 39 (1983) 27–29
[20] C.J. Vales-Pinzon, J.J. Alvarado-Gil, R. Medina-Esquivel, P. Martinez-Torres, Polarized light transmission in ferrofluids loaded with carbon nanotubes in the presence of a uniform magnetic field, J. Magn. Magn. Mater. 369 (2014) 114–121
[21] R. Ellahi, M.H. Tariq, M. Hassan, K. Vafai, On boundary layer nano-ferroliquid flow under the influence of low oscillating stretchable rotating disk. J. Mol. Liq. 229 (2019) 339–345
[22] J.L. Neuringer, Some viscous flows of a saturated ferrofluid under the combined influence of thermal and magnetic field gradients, Int. J. Nonlinear Mech. 1 (1966) 123–137
[23] M. Sheikholeslami, M. Gorji-Bandpy, Free convection of ferrofluid in a cavity heated from below in the presence of an external magnetic field, Powder Technol. 256 (2014) 490–498
[24] S.U. Rehman, A. Zeeshan, A. Majeed, M.B. Arain, Impact of Cattaneo-Christov heat flux model on the flow of Maxwell ferromagnetic liquid along a cold flat plate embedded with two equal magnetic dipoles, J. Magn. 22 (2017) 472–477
[25] M. Hassan, A. Zeeshan, A. Majeed, R. Ellahi, Particle shape effects on ferrofuids flow and heat transfer under influence of low oscillating magnetic field. J. Magn. Magn. Mater. 443 (2017) 36–44
[26] W. Feng, C. Wu, F. Guo, D. Li, Acoustically controlled heat transfer of ferromagnetic fluid, Int. J. Heat Mass Transf. 44 (2001) 4427–4432
[27] M.M. Rashidi, M. Nasiri, M. Khezerloo, N. Laraqi, Numerical investigation of magnetic field effect on mixed convection heat transfer of nanofluid in a channel with sinusoidal walls, J. Magn. Magn. Mater. 93 (2016) 674–6826
[28] M. Sheikholeslami, M. Gorji-Bandpy, Free convection of ferrofluid in a cavity heated from below in the presence of an external magnetic field, Powder Technol. 256 (2014) 490–498
[29] T. Franklin, C. Rinaldi, J.W. Bush, M. Zahn, Deformation of ferrofluid sheets due an applied magnetic field transverse to jet flow, J. Vis. 7 (2004) 175–175
[30] C. Rinaldi, M. Zahn, Ferrohydrodynamic instabilities in dc magnetic fields, J. Vis. 7 (2004) 8–8

[31] C. Lorenz, C. Rinaldi, M. Zahn, Hele-Shaw ferrohydrodynamics for simultaneous in-plane rotating and vertical DC magnetic fields, J. Vis. 7 (2004) 109–109
[32] A. Zavos, P.G. Nikolakopoulos, Computational fluid dynamics analysis of top compression ring in mixed lubrication, Mech. Ind. 18 (2017) 208
[33] M. Muthtamilselvan, S. Sureshkumar, Impact of aspect ratio on a nanofluid-saturated porous enclosure, Mech. Ind. 18 (2017) 501
[34] R. Ellahi, M. Raza, N.S. Akbar, Study of peristaltic flow of nanofluid with entropy generation in a porous medium, J. Porous Media 20 (2017) 461–478
[35] T. Strek, H. Jopek, Computer simulation of heat transfer through a ferrofluid, Phys. Status Solidi (b) 244 (2007) 1027–1037
[36] A. Majeed, A. Zeeshan, R.S.R. Gorla, Convective heat transfer in a dusty ferromagnetic fluid over a stretching surface with prescribed surface temperature/heat flux including heat source/sink, J. Natl. Sci. Found. Sri Lanka 46 (2018) 399–409.
[37] A. Zeeshan, A. Majeed, R. Ellahi, Q.M.Z. Zia, Mixed convection flow and heat transfer in ferromagnetic fluid over a stretching sheet with partial slip effects, Therm. Sci. 22 (2018) 2515–2526.
[38] A. Majeed, A. Zeeshan, T. Hayat, Analysis of magnetic properties of nanoparticles due to applied magnetic dipole in aqueous medium with momentum slip condition, Neural Comp. Appl. 31 (2019) 189–197
[39] H.I. Andersson, O.A. Valnes, Flow of a heated Ferrofluid over a stretching sheet in the presence of a magnetic dipole, Acta Mech. 128 (1998) 39–47

Cite this article as: A. Majeed, A. Zeeshan, F.M. Noori, U. Masud, Influence of rotating magnetic field on Maxwell saturated ferrofluid flow over a heated stretching sheet with heat generation/absorption, Mechanics & Industry **20**, 502 (2019)